

MIR4435-2HG, miR-125b-5p, and Sema4D axis affects the aggressiveness of colorectal cancer cells

Ming Yu, Zhengguo Yi, Shenghui Chen, Xiaopeng Chen, Xiaofeng Xie*

Department of General Surgery (Two), Shangrao Municipal Hospital, Shangrao, Jiangxi 334000, P.R. China

Abstract

Introduction. The purpose of this study is to elucidate the impact of long non-coding RNA (lncRNA) MIR4435-2HG/microRNA (miR)-125b-5p/ Semaphorins 4D (Sema4D) on colorectal cancer (CRC) cell propagation and migration.

Material and methods. Sema4D expression in 73 pairs of CRC tissues and matched adjacent normal tissues was measured by qRT-PCR and western blot and its association with pathological characteristics of CRC patients was analyzed by chi-square test. Also, the expression of MIR4435-2HG, miR-125b-5p and Sema4D in CRC cell lines was detected by qRT-PCR and Western blot. Knockdown or overexpression of MIR4435-2HG, miR-125b-5p and Sema4D were separately performed in Caco-2 and LoVo cells, and the cell propagation, migration and invasiveness were detected by cell-counting kit 8, scratch, and transwell assays.

Results. lncRNA MIR4435-2HG and Sema4D were highly expressed, while miR-125b-5p expression was decreased in CRC tissues and cells. Knockdown of MIR4435-2HG/Sema4D or overexpression of miR-125b-5p inhibited CRC cell proliferation and aggressiveness; overexpression of MIR4435-2HG/Sema4D or knockdown of miR-125b-5p prompted the malignant behaviors of cancer cells. MIR4435-2HG and Sema4D competitively bound to miR-125b-5p.

Conclusions. lncRNA MIR4435-2HG targets miR-125b-5p to upregulate Sema4D expression, and thus regulates CRC cell propagation, migration and invasiveness. (*Folia Histochemica et Cytobiologica* 2022, Vol. 60, No. 2, 191–202)

Keywords: colorectal cancer; humans; cell lines; proliferation; migration; invasion; survival analysis

Introduction

Colorectal cancer (CRC) is the third most commonly diagnosed cancer and the second leading cause of death from cancer worldwide [1–3]. The main cause of CRC-related death is distant invasion and metastasis to the liver, lung, and bone [4]. The available therapies for CRC, including surgery, chemotherapy, radiotherapy, and immunotherapy, are developed, and disappointingly, the efficiency is often restrained by the high metastatic capability and drug resistance during treatment [5, 6]. The facts highlight the importance of

a better understanding of the mechanism responsible for tumor metastasis and invasion.

Long non-coding RNAs (lncRNAs) are defined as a subset of ncRNAs with more than 200 nucleotides in length that could regulate CRC progression and the therapeutic efficacy [7–9]. lncRNA MIR4435-2HG was demonstrated to be increasingly expressed in CRC [10], and its upregulation could promote CRC growth and liver metastasis [11]. Mechanically, lncRNAs could act through competitive endogenous RNA (ceRNA) regulatory networks, that is, they competitively bind with microRNAs (miRs) to sequester the miRs and change the expression levels of their downstream target genes [12]. The regulation of CRC progression by lncRNAs, such as lncRNA nuclear receptor 4 A1, lncRNA MALAT1, and lncRNA RAD51-AS1, through ceRNA networks, has been well documented in previous works [13–15].

*Correspondence address: Xiaofeng Xie

Department of General Surgery (Two), Shangrao Municipal Hospital, No. 72, Wusan Road, Xinzhou Disreict, Shangrao, Jiangxi 334000, P.R. China
phone: 86-13907039812
e-mail: xiexiaofeng454335@163.com

Given that MIR4435-2HG has a pivotal role in CRC, the precise molecular mechanisms still have much to be investigated. Semaphorins 4D (Sema4D) belonging to the class IV semaphorins is capable of regulating tumor growth and vascularity in CRC [16]. The promotive effects of Sema4D on tumor metastasis have also been found in multiple cancers, such as lung cancer, head and neck squamous cell carcinoma, and cutaneous squamous cell carcinoma [17–19]. Sema4D could be regulated by a circular RNA *via* ceRNA mechanism to function its tumor-promoting effect in esophageal squamous cell carcinoma [20]. Interestingly, a bioinformatics tool predicts a possible interaction among lncRNA MIR4435-2HG, miR-125b-5p, and Sema4D. miR-125b-5p is widely considered a tumor-suppressor in colon cancer [21, 22]. miR-125b-5p-mediated chemosensitivity of colon cancer cells to cisplatin could be sequestered by lncRNA DANCR through ceRNA regulatory mechanism [23]. To characterize the mechanisms of MIR4435-2HG regulating CRC progression, we boldly speculated that MIR4435-2HG, through competitively occupying the shared binding sequence of miR-125b-5p, mediated the expression of Sema4D, thus regulating CRC cell aggressiveness.

Material and methods

TCGA database. UALCAN website (<http://ualcan.path.uab.edu/index.html>) was applied to analyze Sema4D gene expression in colon cancer and rectal cancer tissue samples in TCGA database. Sema4D gene expression in multiple tumor cell lines was analyzed using CCLE database (<https://portals.broadinstitute.org/ccle>).

Cells. CRC cell lines (Caco-2, DLD-1, HCT116, LoVo and NCL-H498) and human colonic epithelial cells (NCM460) from American Type Culture Collection (ATCC, Manassas, Virginia, USA) were maintained at 37°C with 5% CO₂ in Dulbecco's modified Eagle's medium (DMEM, Gibco, Grand Island, NY, USA) supplemented with 10% fetal bovine serum (FBS) and 1% penicillin/streptomycin.

CRC tissues. CRC tissues (n = 73) and matched adjacent normal tissues were acquired from CRC patients in Shangrao Municipal Hospital and all CRC tissue samples were diagnosed as CRC after the pathological examination. All the subjects did not receive radiotherapy or chemotherapy before surgery. The samples were rapidly preserved in liquid nitrogen for later use. Acquisition of the tissues was allowed by the ethics committee of Shangrao Municipal Hospital, and informed consent had been obtained from the patients. All the experiments concerning humans complied

Table 1. Clinical data of 73 colorectal cancer patients

	Number
Age	
≤ 60	45
> 60	28
Sex	
Male	39
Female	34
Primary tumor location	
Colon	43
Rectum	30
TNM stage	
I-II	46
III-IV	27
Differentiated degree	
Poor	20
Moderate or well	53
Location of metastases	
Liver	34
Lung	24
Lymph nodes	31
Peritoneal	6

TNM — tumor node metastasis.

with the Declaration of Helsinki. The clinical data of the 73 CRC patients are detailed in Table 1.

qRT-PCR. Total RNA was isolated using TRIZOL (Invitrogen, Carlsbad, CA, USA) and reverse-transcribed by using a reverse transcription kit (TaKaRa, Tokyo, Japan). Gene expressions were quantified using LightCycler 480 fluorescent quantitative PCR instrument (Roche, Indianapolis, IN, USA) per the instruction of the fluorescent quantitative PCR kit (SYBR Green Mix, Roche Diagnostics). Thermal parameters were 95°C for 10 s; 95°C for 5 s, 60°C for 10 s, 72°C for 10 s (a total of 45 cycles); extension at 72°C for 5 min. Each qPCR was performed in triplicate, and U6 was utilized to normalize miR-125b-5p expression and glyceraldehyde-3-phosphate dehydrogenase (GAPDH) to standardize the expression of MIR4435-2HG-F and Sema4D. Data were analyzed through the 2^{-ΔΔCt} method, and the formula was: $\Delta\Delta Ct = (Ct_{\text{target gene}} - Ct_{\text{internal control}})_{\text{experimental group}} - (Ct_{\text{target gene}} - Ct_{\text{internal control}})_{\text{control group}}$. The names of genes and their amplified primers are quoted in Table 2.

Western blotting. Protein was harvested from cells lysed with RIPA lysis buffer (Beyotime), and the concentration

Table 2. Genes and their amplified primers

Name of primer	Sequences
miR-125b-5p-F	TCCCTGAGACCCTAAC
miR-125b-5p-R	TGGTGTCTGGAGTCG
U6-F	CGGGTTTGTTCATTCT
U6-R	AGTCCCAGCATGAACAGCTT
MIR4435-2HG-F	TGCCAGAAAATCTCGTGCCT
MIR4435-2HG-R	TCAAATCCTTGCTGTGCCT
Sema4D-F	GGTCCTGGGGCTCATCTCTA
Sema4D-R	GTGTGCTATTGCAGATGCGG
GAPDH-F	AATGGGCAGCCGTTAGGAAA
GAPDH-R	GCGCCAATACGACCAAATC

F — forward; R — reverse.

was evaluated by using a BCA kit (Beyotime). Then, the protein was homogenized with an equal volume of loading buffer (Beyotime) and degraded through a boiling water bath for 3 min. Then, electrophoresis was run to separate the protein at 80 V for 30 min and switched to 120 V for 1 ~ 2 h. The protein was transferred onto membranes through an ice bath at 300 mA for 60 min, and after being washed for 1 ~ 2 min, the membranes were blocked for 60 min at room temperature or at 4°C overnight. Primary antibodies against GAPDH (5174S, 1:1000) and Sema4D (53108S, 1:1000) (Cell Signaling, Boston, USA) were added for 1-h incubation on a shaking table at room temperature, and the membranes were then washed for 3 × 10 min. Then the membranes were blotted by secondary antibody (14708S, 1:2000, Cell Signaling) for 1 h at room temperature prior to 3 × washing, 10 min each time. Finally, the membranes were visualized using a chemiluminescence image system (Bio-Rad, Hercules, CA, USA) after being developed with the chemiluminescent reagent.

Cell transfection. pcDNA3.1-Sema4D (pcDNA3.1 is an overexpression vector used for Sema4D overexpression), sh-Sema4D (short hairpin RNA for silencing Sema4D), pcDNA3.1-MIR4435-2HG (MIR4435-2HG overexpression vector), sh-MIR4435-2HG (short hairpin RNA for silencing MIR4435-2HG), miR-125b-5p mimic, miR-125b-5p inhibitor and their negative controls (NCs) from GenePharma Co., Ltd (Shanghai, China) were introduced into cells based on

the instructions of Lipofectamine 2000 reagent (Invitrogen, Carlsbad, CA, USA).

CCK-8 assay. After transfection for 24 h, Caco-2 and LoVo cells were seeded onto 96-well plates and 100 μL of diluted cell suspension (1×10^5 cells/mL) was added to each well. Each sample was seeded in triplicate. After being placed in an incubator for 0 h, 24 h, 48 h, 72 h, or 96 h, the cells in each well were immersed in 10 μL of CCK-8 reagent (Tokyo, Dojindo, Japan), and following further incubation for 2 h, the absorbance was obtained at 450 nm wavelength by a microplate spectrophotometer (VSERSA Max, Molecular Devices, California, CA, USA).

Colony formation assay. Caco-2 and LoVo cells were digested by trypsin and centrifuged at 25°C and 1,500 rpm for 5 min. Thereafter, the cells were resuspended in a complete medium. Then, 500 cells/well were seeded onto 6-well plates containing 2 mL of pre-warmed (37°C) complete medium and cultured at 37°C and 5% CO₂ for 2 ~ 3 weeks. The incubation was terminated, and the medium was removed once the colony formation could be seen by eyes. After washing twice with phosphate-buffered saline (PBS), cells were fixed with methanol (1.5 mL/well) for 15 min, and then the methanol was discarded. The cells were stained with 1 mL of Giemsa stain for 20 min in dark. After being washed with running water, the cells were aired and the number of colonies with more than 10 cells was counted under a low-power microscope.

Scratch assay. Transfected Caco-2 and LoVo cells (2×10^6 cells/well) were seeded onto 6-well plates and maintained in an incubator (37°C, 5% CO₂) for 24 h. Each sample was seeded in triplicate. Until the cells covered the bottom of the plates, a sterile 200 μL pipette tip was used to scratch the confluent cells. After PBS wash, the cells were cultured at 37°C and 5% CO₂ for another 24 h. The distance of the scratch was measured at 0 h and 24 h to analyze the migration rate. Migration rate = (the distance of the scratch at 0 h — the distance of the scratch at 24 h)/the distance of the scratch at 0 h.

Transwell invasion assay. Caco-2 and LoVo cells were starved for 24 h in a serum-free medium before disassociation and 2 × PBS washing. The cells were resuspended in a serum-free medium to adjust cell concentration. Twenty-four-well plates and 8-μm Transwell filters (Corning, NY, USA) were used in this assay. The Transwell filters were added with 50 μL Matrigel (Sigma, USA), and each group had three replicate chambers. Then, 100 μL cell suspension (3×10^5 cells) was pipetted onto a matrigel-covered apical chamber (354480, Corning), and a 600 μL medium containing 10% FBS was pipetted into the basolateral chamber. Following incubation at 37°C for 24 h, the medium and

noninvasive cells in the bottom of the apical chamber were removed. Thereafter, the cells were cultured with 4% paraformaldehyde for 30 min and Giemsa for 20 min. Invaded cells were counted by an inverted microscope (Leica DMi8-M, Germany) from 5 random fields. Each experiment was repeated three times.

RNA immunoprecipitation (RIP). Caco-2 cells were collected and then washed with pre-cooled PBS twice prior to centrifugation at 1,500 rpm for 5 min. Thereafter, the cells were homogenized with an equal volume of RIP lysate. Magnetic beads were resuspended in 100 μ L of RIP wash buffer and added with 5 μ g of Ago2 antibody (ab186733, 1:30, Abcam, Cambridge, MA, USA) for 30 min of incubation (room temperature), with IgG antibody as the negative control. The centrifuge tubes were placed on the magnetic rack to discard the supernatant. RIP washing buffer (500 μ L) was added and vibrated before the supernatant was discarded, which was repeated once. Then, 500 μ L of RIP wash buffer was added and vibrated, after which the tubes were maintained on ice. The prepared magnetic beads were added into centrifuge tubes and then placed on a magnetic rack. The supernatant was removed before 900 μ L of RIP immunoprecipitation buffer was added. The unfrozen cell lysate was centrifuged (4°C) at 14,000 rpm for 10 min, and 100 μ L of the supernatant was then pipetted into bead-antibody complexes for incubation at 4°C overnight. Then the tubes were shortly centrifuged and placed on a magnetic rack to remove the supernatant, after which 500 μ L of RIP wash buffer was added. After vibration, the tubes were fixed on the magnetic rack to remove the supernatant and then washed six times. The complexes resuspended in 150 μ L of proteinase K buffer were maintained at 55°C for 30 min. Thereafter, the tubes were fixed on the magnetic rack to collect the supernatant. Gene expressions were evaluated by qRT-PCR after RNA extraction.

Dual-luciferase reporter assay. StarBase was applied to predict the binding site between MIR4435-2HG and miR-125b-5p or between miR-125b-5p and Sema4D, and the wild or mutated sequence of the binding site (WT-MIR4435-2HG, MT-MIR4435-2HG, WT-Sema4D, and MT-Sema4D) was synthesized and cloned into the luciferase reporter vectors (pGL3-Promoter). Thereafter, the vectors were transfected with miR-125b-5p mimic (50 nM) or mimic NC into HEK293T cells. After transfection, firefly luciferase activity and renilla luciferase activity were examined, with renilla luciferase activity as internal reference. Relative activity was the ratio of firefly luciferase activity to renilla luciferase activity.

Statistical analysis. Statistical analysis was performed on GraphPad Prism 8.0 Software and data were exhibited as average \pm standard deviations (average \pm SDs). Two-

group comparisons and multiple-group comparisons were carried out by nonparametric tests Mann-Whitney test and Kruskal-Wallis test, respectively. Kaplan-Meier survival analysis was employed to detect the relationship between Sema4D expression and prognosis of CRC patients, and the chi-square test examined the associations between the pathological characteristics of CRC patients and Sema4D expression. A P value < 0.05 denotes statistical significance.

Results

Increased Sema4D expression in CRC

The TCGA database analysis revealed that Sema4D gene was overexpressed in patients with colon cancer and rectal cancer (Fig. 1A). In the collected 73 pairs of CRC and matched adjacent normal tissues, Sema4D mRNA and protein were upregulated in the carcinoma group compared to the para-carcinoma group (Figs. 1B, 1C). Then, the chi-square test was used to analyze the relevance of Sema4D protein expression with the clinicopathological characteristics of the subjects. The subjects were divided into Sema4D low group (n = 36) and Sema4D high group (n = 37) based on the median of Sema4D protein expression (1.35). The results revealed that Sema4D protein level was closely associated with tissue differentiation (P = 0.0172) and lymph node metastasis (P = 0.0323) (Table 3), while Sema4D protein expression showed no relevance with age, sex, and TNM staging (Table 3).

Kaplan-Meier survival analysis reported that the five-year survival rate was shorter for patients with higher Sema4D protein expression than that for patients with lower Sema4D protein expression (Fig. 1D). CCLE database (<https://portals.broadinstitute.org/ccle>) suggested that Sema4D was generally overexpressed in CRC cell lines (Fig. 1E). Then, Sema4D expression was examined in CRC cell lines (Caco-2, DLD-1, HCT116, LoVo and NCL-H498) and human colon epithelial cells (NCM460). qRT-PCR and Western blotting revealed upregulated Sema4D expression in listed CRC cell lines (Fig. 1F, G). Among the listed CRC cell lines, Caco-2 and LoVo cells showed higher Sema4D protein expression than other CRC cell lines, and thus these two cell lines were selected for subsequent experiments. Altogether, Sema4D was increasingly expressed in CRC tissues and cells and correlated with clinicopathological characteristics of CRC patients.

Upregulated Sema4D in CRC cells promotes cell propagation and aggressiveness

Caco-2 and LoVo cells were transfected with sh-Sema4D or pcDNA3.1-Sema4D, and the results showed that Sema4D expression was decreased in the sh-Se-

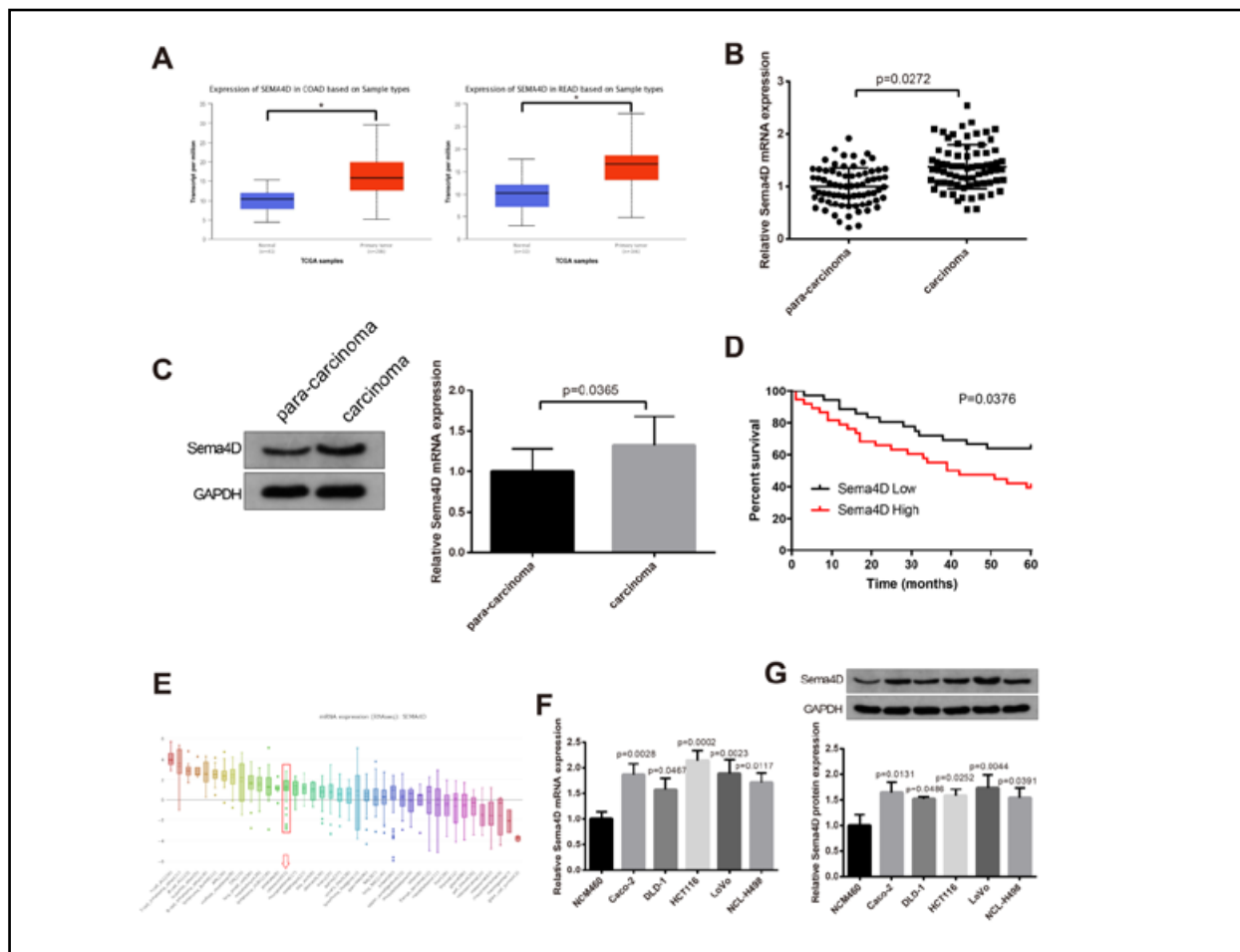


Figure 1. Upregulation of Sema4D in colorectal cancer (CRC) tissues and cell lines. UALCAN website (<http://ualcan.path.uab.edu/index.html>) suggested that Sema4D was highly expressed in colon cancer and rectal cancer samples from TCGA database (A); qRT-PCR (B) and Western blotting (C) of Sema4D expression in CRC tissues and matched adjacent normal tissues; D. Kaplan-Meier survival analysis evaluated the relationship between Sema4D expression and 5-year survival rate of CRC patients (x axis: months); E. CCLE database (<https://portals.broadinstitute.org/ccle>) suggested Sema4D expression in tumor cell lines. qRT-PCR (F) and Western blotting (G) examined Sema4D expression in CRC cell lines. Abbreviations: CCLE — Cancer Cell Line Encyclopedia; CRC — colorectal cancer; Sema4D — Semaphorins 4D; TCGA — the Cancer Genome Atlas.

Table 3. Relevance between Sema4D expression and CRC pathological characteristics

Pathological characteristics	Sema4D Low (36)	Sema4D High (37)	P
Gender (F/M)	16/20	18/19	0.8158
Age	51 ± 13	48 ± 14	0.3463
TNM (I-II/III-IV)	25/11	21/16	0.3342
Differentiated degree (poor/moderate or well)	5/31	15/22	0.0172*
Lymph node metastasis (no/yes)	25/11	17/20	0.0323*

F — female; CRC — colorectal cancer; M — male; Sema4D — Semaphorins 4D; TNM — tumor-node-metastasis. *P < 0.05.

ma4D group compared to that in the sh-NC group, and its expression was increased in the pcDNA3.1-Sema4D group in contrast with pcDNA3.1 group (Figs. 2A, 2B). Then CCK-8 assay showed that Caco-2 and LoVo cell viability was reduced when Sema4D was silenced, and the cell viability was elevated when Sema4D was overexpressed (Fig. 2C). Colony formation assay recapitulated that Sema4D silencing resulted in a decrease of colony number, and inversely the transfection of pcDNA3.1-Sema4D led to an increase of colony number (Fig. 2D). Stractch and Transwell invasion assays indicated that the invasion and migration rates of Caco-2 and LoVo cells were increased in the pcDNA3.1-Sema4D group and decreased in the sh-Sema4D group (Figs. 2E, 2F). Collectively, silencing of Sema4D inhibited CRC cell behaviors

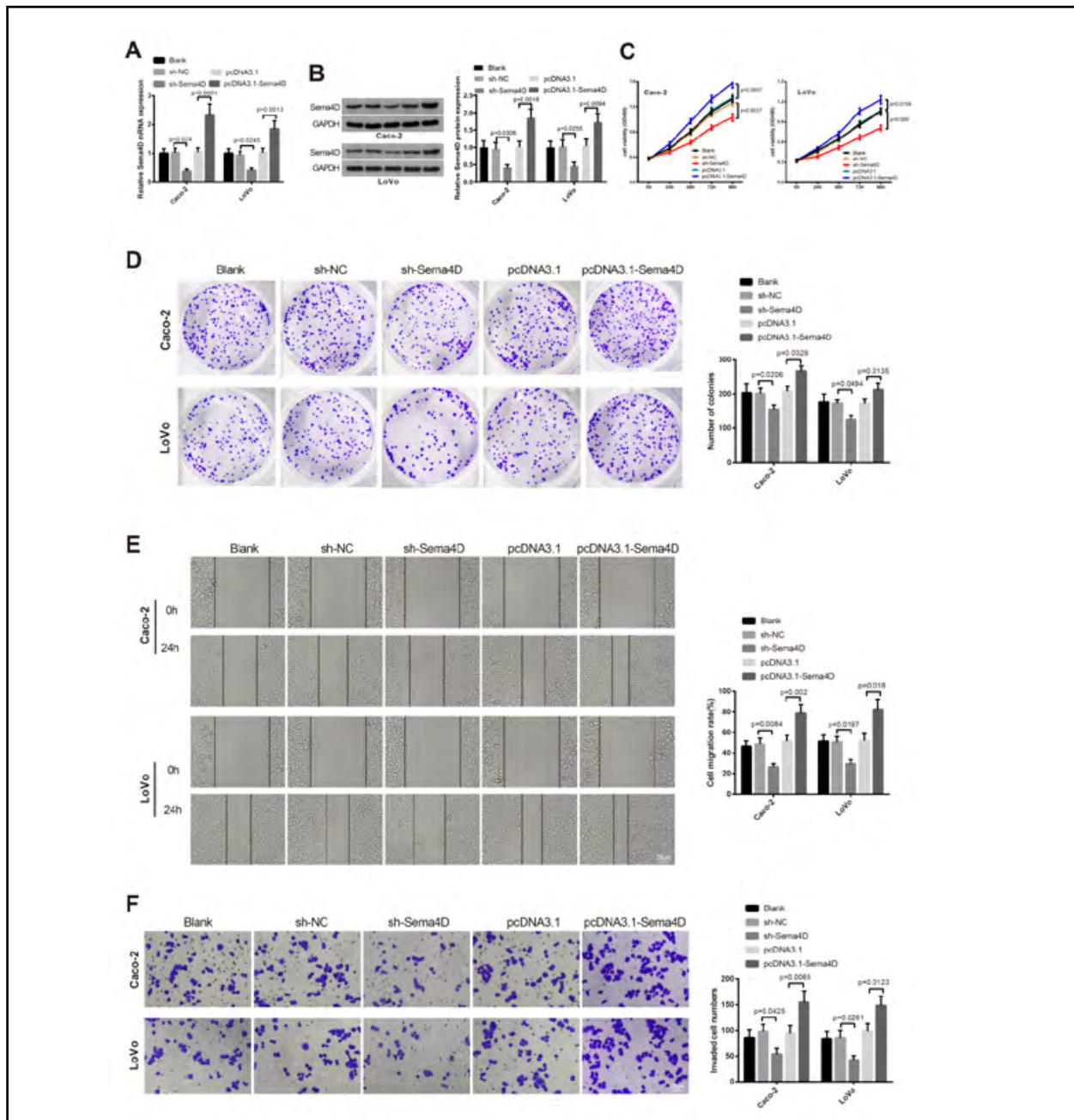


Figure 2. Increasingly expressed Sema4D in CRC cells prompts cell proliferation, migration and invasion. Sema4D expression in CRC cells as measured by qRT-PCR (A) and western blotting (B); C. CCK-8 assay measured cell viability; D. Colony formation assay evaluated cell proliferation; E. Scratch assay assessed the migration rate of CRC cells; F. Invasiveness of cells was detected through Transwell invasion assay. Abbreviations: CRC — colorectal cancer; Sema4D — Semaphorins 4D.

(i.e., proliferation, migration and invasion) but overexpression of Sema4D promoted CRC cell progression.

miR-125b-5p targets Sema4D to inhibit CRC cell proliferation, migration and invasion

The detection of miR-125b-5p expression using qRT-PCR suggested the downregulated expression of miR-125b-5p in CRC tissues and cell lines (Figs. 3A,

3B). The binding between Ago2 and Sema4D mRNA was identified by RIP assay. In Caco-2 cells, AGO2 antibody could enrich Sema4D mRNA (Fig. 3C). There was a binding site between miR-125b-5p and Sema4D in StarBase (<http://starbase.sysu.edu.cn/>) (Fig. 3D). In addition, the dual luciferase reporter assay corroborated that miR-125b-5p mimic reduced the luciferase activity in the WT-Sema4D group, and

the luciferase activity in the MT-Sema4D group was not changed by the miR-125b-5p mimic (Fig. 3E), supporting that miR-125b-5p bound to Sema4D.

Next, to characterize the role of miR-125b-5p/Sema4D axis in CRC cells, Caco-2 and LoVo cells were transfected with miR-125b-5p mimic, miR-125b-5p inhibitor or miR-125b-5p mimic + pcDNA3.1-Sema4D, and the cell behaviors, *i.e.*, proliferation, migration and invasion, were evaluated. qRT-PCR results showed that transfection of miR-125b-5p mimic elevated miR-125b-5p expression in Caco-2 and LoVo cells, and miR-125b-5p level was reduced in the cells transfected with miR-125b-5p inhibitor (Fig. 3F). As measured by qRT-PCR and Western blotting, Sema4D expression in Caco-2 and LoVo cells declined after transfection of miR-125b-5p mimic, and transfection of miR-125b-5p inhibitor rescued Sema4D expression (Figs. 3G, 3H). Caco-2 and LoVo cells overexpressing miR-125b-5p showed weakened cell viability and colony formation ability in addition to decreased migration rate and invasiveness, but these effects were minimized when Sema4D was overexpressed despite upregulated miR-125b-5p (Figs. 3I–3L). Results were reversed (*i.e.*, strengthened cell viability and colony formation ability and increased migration and invasion rates) when miR-125b-5p was inhibited (Figs. 3I–3L). Altogether, miR-125b-5p overexpression suppressed the malignant behaviors of CRC cells by targeting Sema4D.

LncRNA MIR4435-2HG enhances CRC cell propagation and aggressiveness through miR-125b-5p

Firstly, we analyzed lncRNA MIR4435-2HG expression in the TCGA database, and the results suggested increasingly expressed MIR4435-2HG in CRC tissues (Fig. 4A, $P < 0.05$). MIR4435-2HG expression in 73 pairs of CRC and normal adjacent tissues was examined by qRT-PCR. As expected, our data proved that MIR4435-2HG was upregulated in CRC tissues and cells (Figs. 4B, 4C). RIP results presented that the AGO2 antibody could enrich MIR4435-2HG in Caco-2 cells (Fig. 4D). StarBase (<http://starbase.sysu.edu.cn/>) predicted a binding site between MIR4435-2HG and miR-125b-5p (Fig. 4E). According to the results of dual-luciferase reporter assay, transfection with miR-125b-5p mimic reduced the luciferase activity of the WT-MIR4435-2HG group, and the luciferase activity was not altered in MT-MIR4435-2HG group (Fig. 4F). As suggested by the aforementioned results, lncRNA MIR4435-2HG and Sema4D could competitively bind to miR-125b-5p.

To examine the effects of lncRNA MIR4435-2HG/miR-125b-5p axis in CRC cells, Caco-2 and LoVo cells were transfected with sh-MIR4435-2HG, pcDNA3.1-

MIR4435-2HG or sh-MIR4435-2HG + miR-125b-5p inhibitor. The results of qRT-PCR manifested that transfection of sh-MIR-4435-2HG downregulated MIR4435-2HG expression while elevating miR-125b-5p expression in the cells, and transfection of pcDNA3.1-MIR4435-2HG increased MIR4435-2HG expression but lowered miR-125b-5p expression (Fig. 4G). Compared to sh-MIR-4435-2HG group, sh-MIR4435-2HG + miR-125b-5p inhibitor group showed a decrease of miR-125b-5p expression (Fig. 4G). Transfection of sh-MIR4435-2HG reduced the cell viability, migration rate, colony formation ability, and invasiveness of Caco-2 and LoVo cells, and transfection of pcDNA3.1-MIR4435-2HG enhanced the aforementioned biological behaviors (Figs. 4H–4K). Moreover, the cell viability, colony formation ability, migration rate, and invasiveness of Caco-2 and LoVo cells were promoted when miR-125b-5p was inhibited in spite of silenced MIR4435-2HG (Fig. 4H–K). Overall, lncRNA MIR4435-2HG enhanced the proliferation and the aggressive phenotype of CRC cells through upregulating Sema4D by decoying miR-125b-5p.

Discussion

Accumulating evidence has reported that MIR4435-2HG is implicated in the onset and development of various types of tumors [24, 25]. The goal of the present study was to reveal whether lncRNA MIR4435-2HG could mediate CRC development by upregulating Sema4D expression through sequestering miR-125b-5p. In the present work, MIR4435-2HG plays an oncogenic role in CRC development by relieving the inhibition of miR-125b-5p on Sema4D, which contributes to a deeper insight into gene-regulatory mechanisms associated with MIR4435-2HG-induced cell migration and invasion.

First of all, we unveiled that increased Sema4D expression in CRC tissues was tightly associated with adverse pathological characteristics and a poor 5-year survival rate in CRC patients, which is in line with the findings in other cancers such as epithelial ovarian cancer and gastric carcinoma [26, 27]. A previous study also stated that overexpression of Sema4D is positively correlated with the advancement in lymphatic metastasis, the TNM stage, the differentiation status of the tumor and survival time for CRC patients [28]. These findings demonstrated that Sema4D might be an indicator for CRC progression. In cellular experiments, the Sema4D overexpressing CRC cells showed strengthened potentials for proliferation, invasiveness, and migration, and Sema4D knockdown significantly suppressed the aggressive

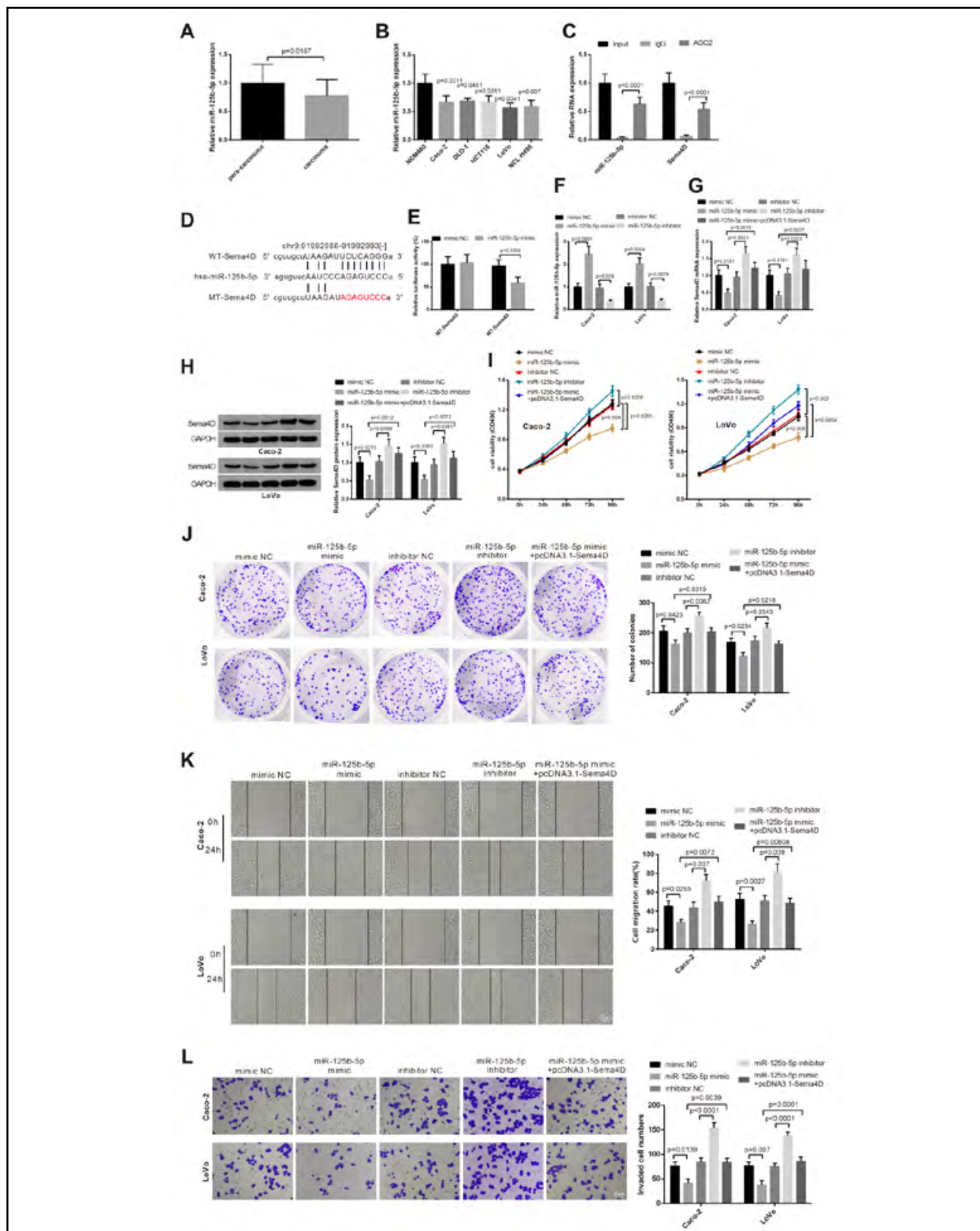


Figure 3. miR-125b-5p inhibits CRC cell proliferation, migration and invasion by acting on Sema4D. MiR-125b-5p expression in tumor tissue of CRC patients (A) and CRC cell lines (B) as detected by qRT-PCR; C. Direct binding between miR-125b-5p and Sema4D as measured by RIP assay; D. A binding site of miR-125b-5p and Sema4D was determined according to StarBase; E. The binding between miR-125b-5p and Sema4D was identified by dual luciferase reporter assay; F. Following transfection of miR-125b-5p mimic, miR-125b-5p inhibitor or miR-125b-5p mimic + pcDNA3.1-Sema4D, qRT-PCR detected miR-125b-5p level. Sema4D expression was measured by qRT-PCR (G) and Western blotting (H). Cell viability was assessed by CCK-8 assay (I), colony formation ability by colony formation assay (J), migration rate by scratch assay (K), and invasiveness by Transwell invasion assay (L). CRC — colorectal cancer; RIP — RNA immunoprecipitation; Sema4D — Semaphorins 4D.

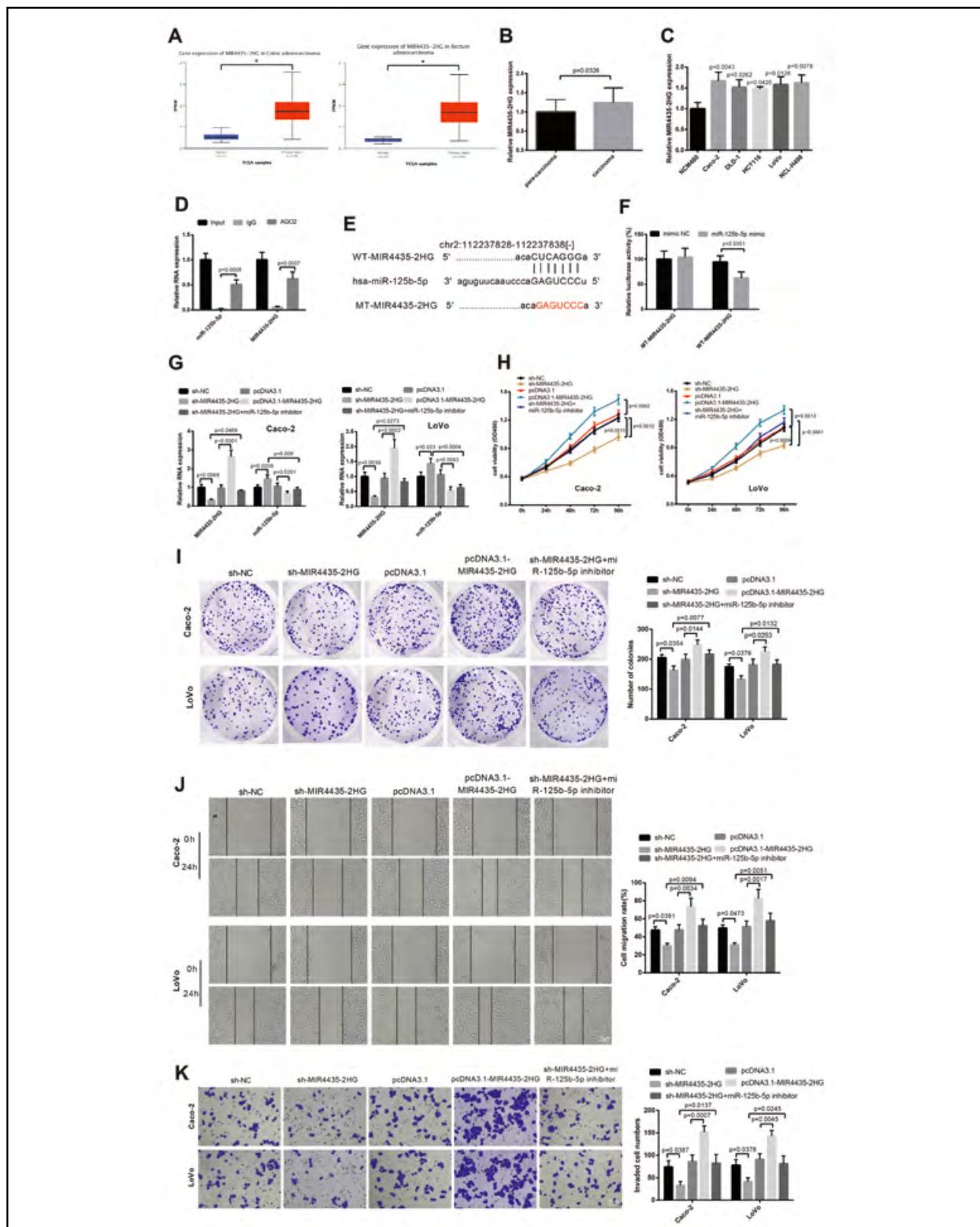


Figure 4. MIR4435-2HG targets miR-125b-5p to act on CRC cells. **A.** MIR4435-2HG expression in colon cancer and rectal cancer from TCGA database in UALCAN website. qRT-PCR analysis of MIR4435-2HG expression in CRC tissues (**B**) and cells (**C**); **D.** The direct binding between MIR4435-2HG and miR-125b-5p as measured by RIP assay; **E.** The binding sites of MIR4435-2HG and miR-125b-5p in StarBase (**E**); The binding of MIR-4435-2HG to miR-125b-5p were identified by dual luciferase reporter assay (**F**); levels of MIR4435-2HG and miR-125b-5p were detected by qRT-PCR (**G**); CCK-8 assay determined the cell viability (**H**); colony formation assay examined the colony formation ability (**I**); Scratch assay detected the migration rate (**J**); Transwell invasion assay assessed the cell invasiveness (**K**). CRC — colorectal cancer; RIP — RNA immunoprecipitation.

phenotype of CRC cells. Previous studies also have reported the oncogenic role of Sema4D in terms of facilitating migratory capacity, vasculogenic mimicry formation, and invasiveness [27, 29, 30]. Despite that Sema4D has been mentioned to promote angiogenesis and invasive growth in CRC through binding to its receptor PlexinB1 [31], the action mechanism being still far from clear.

Then, bioinformatics prediction revealed a binding site between miR-125b-5p and Sema4D. To characterize the action mechanism of Sema4D exacerbating CRC development, functional experiments were conducted and confirmed the binding of miR-125b-5p to Sema4D concurrent with the negative regulation of Sema4D by miR-125b-5p. Ren and colleagues have documented that miR-125b suppressed the tumor aggressiveness induced by subgroup J avian leukosis virus and enhanced apoptosis in chicken by binding to Sema4D [32]. miR-125b-5p was expressed at a low level in CRC tissues and cells, and upregulation of its expression exhibited significant inhibitory effects on CRC cell propagation and aggressiveness. The suppressive effect of miR-125b-5p on cancer development has been referred. For instance, miR-125b-5p could inhibit cervical cancer cell migration and proliferation mediated by lncRNA CAR10 [33]. In CRC cells, miR-125b-5p could reduce the migratory and invasive phenotypes of chemo-resistant cancer cells through binding to Sp1 [34, 35]. Our data proved that the tumor-suppressive effect of miR-125b-5p in CRC cells was partially counteracted by Sema4D overexpression. In the present study, we validated that miR-125b-5p harbored inhibiting effects on the aggressive phenotypes of CRC cells through binding to Sema4D.

As its well known, lncRNA could participate in the biological functions of cells through its binding targets such as miRs and proteins [36]. Therefore, we considered whether a certain lncRNA could regulate the miR-125b-5p/Sema4D axis to participate in the biological processes of CRC cells. In combination with bioinformatics prediction and RIP result, we confirmed that MIR4435-2HG could directly bind to miR-125b-5p. As expected, the expression of MIR4435-2HG was increased in both CRC tissues and cells, and it functioned as an oncogenic gene in CRC, as evidenced by enhanced CRC cell propagation and aggressiveness in response to MIR4435-2HG overexpression. Patients with higher expression of MIR4435-2HG are more likely to have larger tumor size and advanced TNM staging in addition to lymph node metastasis [37]. Besides, the downregulated MIR4435-2HG could not only inhibit CRC cell proliferation but also prompt CRC cell apoptosis [38].

Moreover, MIR4435-2HG has also been confirmed to mediate tumor growth and liver metastasis in CRC by acting as a ceRNA [11]. The current work suggested that the malignant phenotypes of CRC cells were restrained when MIR4435-2HG expression was silenced but overexpression of miR-125b-5p strengthened the proliferation and migration of CRC cells in spite of silenced MIR4435-2HG. Overall, the findings of this study illuminated that MIR4435-2HG regulated Sema4D expression by occupying the shared binding sequence of miR-125b-5p to exacerbate CRC progression. This study highlighting the implication of the MIR4435-2HG/miR-125b-5p/Sema4D axis in tumor metastasis and invasion may provide a chance for controlling CRC development. But the interpretation of the results should be cautious due to the limitations of this study. For instance, the tumor-promoting effect of lncRNA MIR4435-2HG in CRC should be further confirmed in pre-clinical models. The regulatory relationship of lncRNA MIR4435-2HG/miR-125b-5p/Sema4D axis needs to be identified in CRC patients.

In conclusion, this study demonstrated lncRNA MIR4435-2HG knockdown suppressed CRC cell propagation and aggressiveness *via* miR-125b-5p-mediated Sema4D. The research regarding MIR4435-2HG/miR-125b-5p/Sema4D axis provides a possible therapeutic candidate targeting tumor metastasis and invasion for CRC treatment. Meanwhile, a larger number of specimens are required to intensify the clinical significance of the MIR4435-2HG/miR-125b-5p/Sema4D axis in CRC patients for future investigations.

Conflict of interest

The author declares that they have nothing worth disclosure.

References

1. Sung H, Ferlay J, Siegel RL, et al. Global cancer statistics 2020: GLOBOCAN estimates of incidence and mortality worldwide for 36 cancers in 185 countries. *CA Cancer J Clin.* 2021; 71(3): 209–249, doi: [10.3322/caac.21660](https://doi.org/10.3322/caac.21660), indexed in Pubmed: [33538338](https://pubmed.ncbi.nlm.nih.gov/33538338/).
2. Bray F, Ferlay J, Soerjomataram I, et al. Global cancer statistics 2018: GLOBOCAN estimates of incidence and mortality worldwide for 36 cancers in 185 countries. *CA Cancer J Clin.* 2018; 68(6): 394–424, doi: [10.3322/caac.21492](https://doi.org/10.3322/caac.21492), indexed in Pubmed: [30207593](https://pubmed.ncbi.nlm.nih.gov/30207593/).
3. Huang W, Sundquist J, Sundquist K, et al. Use of phosphodiesterase 5 inhibitors is associated with lower risk of colorectal cancer in men with benign colorectal neoplasms. *Gastroenterology.* 2019; 157(3): 672–681.e4, doi: [10.1053/j.gastro.2019.05.012](https://doi.org/10.1053/j.gastro.2019.05.012), indexed in Pubmed: [31103628](https://pubmed.ncbi.nlm.nih.gov/31103628/).
4. Tang Bo, Liang W, Liao Y, et al. PEA15 promotes liver metastasis of colorectal cancer by upregulating the ERK/MAPK signaling pathway. *Oncol Rep.* 2019; 41(1): 43–56, doi: [10.3892/or.2018.6825](https://doi.org/10.3892/or.2018.6825), indexed in Pubmed: [30365128](https://pubmed.ncbi.nlm.nih.gov/30365128/).

5. Kishore C, Bhadra P. Current advancements and future perspectives of immunotherapy in colorectal cancer research. *Eur J Pharmacol.* 2021; 893: 173819, doi: [10.1016/j.ejphar.2020.173819](https://doi.org/10.1016/j.ejphar.2020.173819), indexed in Pubmed: [33347822](https://pubmed.ncbi.nlm.nih.gov/33347822/).
6. Hong S, Yan Z, Wang H, et al. miR-663b promotes colorectal cancer progression by activating Ras/Raf signaling through downregulation of TNK1. *Hum Cell.* 2020; 33(1): 104–115, doi: [10.1007/s13577-019-00294-w](https://doi.org/10.1007/s13577-019-00294-w), indexed in Pubmed: [31758392](https://pubmed.ncbi.nlm.nih.gov/31758392/).
7. Deng X, Ruan H, Zhang X, et al. Long noncoding RNA CCAL transferred from fibroblasts by exosomes promotes chemoresistance of colorectal cancer cells. *Int J Cancer.* 2020; 146(6): 1700–1716, doi: [10.1002/ijc.32608](https://doi.org/10.1002/ijc.32608), indexed in Pubmed: [31381140](https://pubmed.ncbi.nlm.nih.gov/31381140/).
8. Jiang X, Zhu Q, Wu P, et al. Upregulated long noncoding RNA LINC01234 predicts unfavorable prognosis for colorectal cancer and negatively correlates with KLF6 expression. *Ann Lab Med.* 2020; 40(2): 155–163, doi: [10.3343/alm.2020.40.2.155](https://doi.org/10.3343/alm.2020.40.2.155), indexed in Pubmed: [31650732](https://pubmed.ncbi.nlm.nih.gov/31650732/).
9. Shang AQ, Wang WW, Yang YB, et al. Knockdown of long noncoding RNA PVT1 suppresses cell proliferation and invasion of colorectal cancer via upregulation of microRNA-214-3p. *Am J Physiol Gastrointest Liver Physiol.* 2019; 317(2): G222–G232, doi: [10.1152/ajpgi.00357.2018](https://doi.org/10.1152/ajpgi.00357.2018), indexed in Pubmed: [31125260](https://pubmed.ncbi.nlm.nih.gov/31125260/).
10. Wu M, Li W, Huang F, et al. Comprehensive analysis of the expression profiles of long non-coding RNAs with associated ceRNA network involved in the colon cancer staging and progression. *Sci Rep.* 2019; 9(1): 16910, doi: [10.1038/s41598-019-52883-2](https://doi.org/10.1038/s41598-019-52883-2), indexed in Pubmed: [31729423](https://pubmed.ncbi.nlm.nih.gov/31729423/).
11. Dong X, Yang Z, Yang H, et al. Long non-coding RNA MIR4435-2HG promotes colorectal cancer proliferation and metastasis through miR-206/YAP1 axis. *Front Oncol.* 2020; 10: 160, doi: [10.3389/fonc.2020.00160](https://doi.org/10.3389/fonc.2020.00160), indexed in Pubmed: [32154166](https://pubmed.ncbi.nlm.nih.gov/32154166/).
12. Wang L, Cho KB, Li Y, et al. Long noncoding RNA (lncRNA)-mediated competing endogenous RNA networks provide novel potential biomarkers and therapeutic targets for colorectal cancer. *Int J Mol Sci.* 2019; 20(22), doi: [10.3390/ijms20225758](https://doi.org/10.3390/ijms20225758), indexed in Pubmed: [31744051](https://pubmed.ncbi.nlm.nih.gov/31744051/).
13. Li C, Wang P, Du J, et al. LncRNA RAD51-AS1/miR-29b/c-3p/NDRG2 crosstalk repressed proliferation, invasion and glycolysis of colorectal cancer. *IUBMB Life.* 2021; 73(1): 286–298, doi: [10.1002/iub.2427](https://doi.org/10.1002/iub.2427), indexed in Pubmed: [33314669](https://pubmed.ncbi.nlm.nih.gov/33314669/).
14. Liu Z, Gu Y, Cheng X, et al. Upregulation lnc-NEAT1 contributes to colorectal cancer progression through sponging miR-486-5p and activating NR4A1/Wnt/-catenin pathway. *Cancer Biomark.* 2021; 30(3): 309–319, doi: [10.3233/CBM-201733](https://doi.org/10.3233/CBM-201733), indexed in Pubmed: [33337350](https://pubmed.ncbi.nlm.nih.gov/33337350/).
15. Zhang C, Yao K, Zhang J, et al. Long noncoding RNA MALAT1 promotes colorectal cancer progression by acting as a ceRNA of miR-508-5p to regulate RAB14 expression. *Biomol Res Int.* 2020; 2020: 4157606, doi: [10.1155/2020/4157606](https://doi.org/10.1155/2020/4157606), indexed in Pubmed: [33344634](https://pubmed.ncbi.nlm.nih.gov/33344634/).
16. Ding X, Qiu L, Zhang L, et al. The role of semaphorin 4D as a potential biomarker for antiangiogenic therapy in colorectal cancer. *Onco Targets Ther.* 2016; 9: 1189–1204, doi: [10.2147/OTT.S98906](https://doi.org/10.2147/OTT.S98906), indexed in Pubmed: [27022279](https://pubmed.ncbi.nlm.nih.gov/27022279/).
17. Cao J, Zhang C, Chen T, et al. Plexin-B1 and semaphorin 4D cooperate to promote cutaneous squamous cell carcinoma cell proliferation, migration and invasion. *J Dermatol Sci.* 2015; 79(2): 127–136, doi: [10.1016/j.jdermsci.2015.05.002](https://doi.org/10.1016/j.jdermsci.2015.05.002), indexed in Pubmed: [26051877](https://pubmed.ncbi.nlm.nih.gov/26051877/).
18. Chen WG, Sun J, Shen WW, et al. Sema4D expression and secretion are increased by HIF-1 α and inhibit osteogenesis in bone metastases of lung cancer. *Clin Exp Metastasis.* 2019; 36(1): 39–56, doi: [10.1007/s10585-018-9951-5](https://doi.org/10.1007/s10585-018-9951-5), indexed in Pubmed: [30617444](https://pubmed.ncbi.nlm.nih.gov/30617444/).
19. Zhang C, Qiao H, Guo W, et al. CD100-plexin-B1 induces epithelial-mesenchymal transition of head and neck squamous cell carcinoma and promotes metastasis. *Cancer Lett.* 2019; 455: 1–13, doi: [10.1016/j.canlet.2019.04.013](https://doi.org/10.1016/j.canlet.2019.04.013), indexed in Pubmed: [30981760](https://pubmed.ncbi.nlm.nih.gov/30981760/).
20. Zhou S, Guo Z, Zhou C, et al. circ_NRP1 is oncogenic in malignant development of esophageal squamous cell carcinoma (ESCC) via miR-595/SEMA4D axis and PI3K/AKT pathway. *Cancer Cell Int.* 2021; 21(1): 250, doi: [10.1186/s12935-021-01907-x](https://doi.org/10.1186/s12935-021-01907-x), indexed in Pubmed: [33957921](https://pubmed.ncbi.nlm.nih.gov/33957921/).
21. Cenariu D, Zimta AA, Munteanu R, et al. Hsa-miR-125b therapeutic role in colon cancer is dependent on the mutation status of the TP53 gene. *Pharmaceutics.* 2021; 13(5), doi: [10.3390/pharmaceutics13050664](https://doi.org/10.3390/pharmaceutics13050664), indexed in Pubmed: [34066331](https://pubmed.ncbi.nlm.nih.gov/34066331/).
22. Zhang J, Yang W, Xiao Y, et al. MiR-125b inhibits cell proliferation and induces apoptosis in human colon cancer SW480 cells via targeting STAT3. *Recent Pat Anticancer Drug Discov.* 2022; 17(2): 187–194, doi: [10.2174/1574892816666210708165037](https://doi.org/10.2174/1574892816666210708165037), indexed in Pubmed: [34238196](https://pubmed.ncbi.nlm.nih.gov/34238196/).
23. Shi H, Li K, Feng J, et al. LncRNA-DANCR interferes with miR-125b-5p/HK2 axis to desensitize colon cancer cells to cisplatin via activating anaerobic glycolysis. *Front Oncol.* 2020; 10: 1034, doi: [10.3389/fonc.2020.01034](https://doi.org/10.3389/fonc.2020.01034), indexed in Pubmed: [32766131](https://pubmed.ncbi.nlm.nih.gov/32766131/).
24. Wang H, Wu M, Lu Y, et al. LncRNA MIR4435-2HG targets desmoplakin and promotes growth and metastasis of gastric cancer by activating Wnt/ β -catenin signaling. *Aging (Albany NY).* 2019; 11(17): 6657–6673, doi: [10.18632/aging.102164](https://doi.org/10.18632/aging.102164), indexed in Pubmed: [31484163](https://pubmed.ncbi.nlm.nih.gov/31484163/).
25. Yang M, He X, Huang X, et al. LncRNA MIR4435-2HG-mediated upregulation of TGF- β 1 promotes migration and proliferation of non-small cell lung cancer cells. *Environ Toxicol.* 2020; 35(5): 582–590, doi: [10.1002/tox.22893](https://doi.org/10.1002/tox.22893), indexed in Pubmed: [31875359](https://pubmed.ncbi.nlm.nih.gov/31875359/).
26. Chen Y, Zhang L, Liu WX, et al. VEGF and SEMA4D have synergistic effects on the promotion of angiogenesis in epithelial ovarian cancer. *Cell Mol Biol Lett.* 2018; 23: 2, doi: [10.1186/s11658-017-0058-9](https://doi.org/10.1186/s11658-017-0058-9), indexed in Pubmed: [29308068](https://pubmed.ncbi.nlm.nih.gov/29308068/).
27. Li H, Wang JS, Mu LJ, et al. Promotion of Sema4D expression by tumor-associated macrophages: significance in gastric carcinoma. *World J Gastroenterol.* 2018; 24(5): 593–601, doi: [10.3748/wjg.v24.i5.593](https://doi.org/10.3748/wjg.v24.i5.593), indexed in Pubmed: [29434448](https://pubmed.ncbi.nlm.nih.gov/29434448/).
28. Wang JS, Jing CQ, Shan KS, et al. Semaphorin 4D and hypoxia-inducible factor-1 α overexpression is related to prognosis in colorectal carcinoma. *World J Gastroenterol.* 2015; 21(7): 2191–2198, doi: [10.3748/wjg.v21.i7.2191](https://doi.org/10.3748/wjg.v21.i7.2191), indexed in Pubmed: [25717256](https://pubmed.ncbi.nlm.nih.gov/25717256/).
29. Wang Y, Zhao H, Zhi W. SEMA4D under the posttranscriptional regulation of HuR and miR-4319 boosts cancer progression in esophageal squamous cell carcinoma. *Cancer Biol Ther.* 2020; 21(2): 122–129, doi: [10.1080/15384047.2019.1669996](https://doi.org/10.1080/15384047.2019.1669996), indexed in Pubmed: [31651222](https://pubmed.ncbi.nlm.nih.gov/31651222/).
30. Xia Y, Cai XY, Fan JQ, et al. The role of sema4D in vasculogenic mimicry formation in non-small cell lung cancer and the underlying mechanisms. *Int J Cancer.* 2019; 144(9): 2227–2238, doi: [10.1002/ijc.31958](https://doi.org/10.1002/ijc.31958), indexed in Pubmed: [30374974](https://pubmed.ncbi.nlm.nih.gov/30374974/).
31. Ikeya T, Maeda K, Nagahara H, et al. The combined expression of Semaphorin4D and PlexinB1 predicts disease recurrence in colorectal cancer. *BMC Cancer.* 2016; 16: 525, doi: [10.1186/s12885-016-2577-6](https://doi.org/10.1186/s12885-016-2577-6), indexed in Pubmed: [27456345](https://pubmed.ncbi.nlm.nih.gov/27456345/).

32. Ren C, Xie R, Yao Y, et al. MiR-125b suppression inhibits apoptosis and negatively regulates Sema4D in avian leukosis virus-transformed cells. *Viruses*. 2019; 11(8), doi: [10.3390/v11080728](https://doi.org/10.3390/v11080728), indexed in Pubmed: [31394878](https://pubmed.ncbi.nlm.nih.gov/31394878/).
33. Hu T, Zhang Q, Gao L. LncRNA CAR10 upregulates PDPK1 to promote cervical cancer development by sponging miR-125b-5p. *Biomed Res Int*. 2020; 2020: 4351671, doi: [10.1155/2020/4351671](https://doi.org/10.1155/2020/4351671), indexed in Pubmed: [32025520](https://pubmed.ncbi.nlm.nih.gov/32025520/).
34. Park GB, Jeong JY, Kim D. Modified TLR-mediated down-regulation of miR-125b-5p enhances CD248 (endosialin)-induced metastasis and drug resistance in colorectal cancer cells. *Mol Carcinog*. 2020; 59(2): 154–167, doi: [10.1002/mc.23137](https://doi.org/10.1002/mc.23137), indexed in Pubmed: [31746054](https://pubmed.ncbi.nlm.nih.gov/31746054/).
35. Park GB, Jeong JY, Kim D. GLUT5 regulation by AKT1/3-miR-125b-5p downregulation induces migratory activity and drug resistance in TLR-modified colorectal cancer cells. *Carcinogenesis*. 2020; 41(10): 1329–1340, doi: [10.1093/carcin/bgaa074](https://doi.org/10.1093/carcin/bgaa074), indexed in Pubmed: [32649737](https://pubmed.ncbi.nlm.nih.gov/32649737/).
36. Zhan W, Liao X, Chen Z, et al. LINC00858 promotes colorectal cancer by sponging miR-4766-5p to regulate PAK2. *Cell Biol Toxicol*. 2020; 36(4): 333–347, doi: [10.1007/s10565-019-09506-3](https://doi.org/10.1007/s10565-019-09506-3), indexed in Pubmed: [31902050](https://pubmed.ncbi.nlm.nih.gov/31902050/).
37. Shen MY, Zhou GR, -Y Zhang Z. LncRNA MIR4435-2HG contributes into colorectal cancer development and predicts poor prognosis. *Eur Rev Med Pharmacol Sci*. 2020; 24(4): 1771–1777, doi: [10.26355/eurev_202002_20354](https://doi.org/10.26355/eurev_202002_20354), indexed in Pubmed: [32141545](https://pubmed.ncbi.nlm.nih.gov/32141545/).
38. Ouyang W, Ren L, Liu G, et al. LncRNA MIR4435-2HG predicts poor prognosis in patients with colorectal cancer. *PeerJ*. 2019; 7: e6683, doi: [10.7717/peerj.6683](https://doi.org/10.7717/peerj.6683), indexed in Pubmed: [30972258](https://pubmed.ncbi.nlm.nih.gov/30972258/).

Submitted: 27 October, 2021

Accepted after reviews: 10 June, 2022

Available as AoP: 22 June, 2022